Clim Dyn (2015) 44:1645–1659
DOI 10.1007/s00382-014-2402-3

Reconstruction of the springtime East Asian Subtropical Jet and Western Pacific pattern from a millennial-length Taiwanese tree-ring chronology

W. E. Wright · B. T. Guan · Y.-H. Tseng · E. R. Cook · K.-Y. Wei · S.-T. Chang

Received: 4 November 2013 / Accepted: 3 November 2014 / Published online: 12 November 2014

Abstract The East Asian subtropical jet (EAJ) and the closely related Western Pacific pattern (WP) are among the most important features in global atmospheric dynamics, but little is known about their long-term variability. This study presents reconstructions of the Spring EAJ index (EAJI) and the Spring WP index (WPI) based on significant relationships identified between mean values for these features and a millennial length tree-ring width chronology of *Chamaecyparis obtusa* var. *formosana*, a high-mountain cloud forest species from northeastern Taiwan. Tree-ring based reconstructions of high pass filtered versions of the EAJI and WPI (EAJI 5YR and WPI 5YR) presented herein explain 42 and 31 % of the WPI 5YR and EAJI 5YR, respectively, and display acceptable reliability back to A.D. 1237. A significant trend present in the long-term variance of the reconstructed EAJI and WPI after A.D. 1860 suggests long-term increasing variability in the spring mean latitudinal placement and/or the strength/breadth of the EAJ core region near Taiwan and Japan and in the trajectory of the EAJ over the North Pacific. Related features affected by changes in the EAJ include the North Pacific storm track and Asian Dust transport.

Keywords Tree-ring · Cloud forest · East Asian Subtropical jet · Western Pacific pattern · North Pacific storm track · Temperature

Electronic supplementary material The online version of this article (doi:10.1007/s00382-014-2402-3) contains supplementary material, which is available to authorized users.

W. E. Wright (✉)
Laboratory of Tree-Ring Research,
The University of Arizona, Tucson, AZ, USA
e-mail: wwright@LTRR.Arizona.edu

B. T. Guan · S.-T. Chang
School of Forestry and Resource Conservation,
National Taiwan University, Taipei, Taiwan

Y.-H. Tseng
Earth System Laboratory, National Center
for Atmospheric Research, Boulder, CO, USA

E. R. Cook
Biology and Paleoenvironment, Lamont–Doherty
Earth Observatory, Palisades, NY, USA

K.-Y. Wei
Department of Geoscience, National Taiwan University,
Taipei, Taiwan

1 Introduction

Very few high-resolution natural proxy records of subtropical and tropical climate have been developed for the western North Pacific and East/Southeast Asia equatorward of 30°N despite the critical roles played by the East Asian Monsoon, the East Asian Subtropical Jet and the Indonesian warm pool in regional climate and in global climate change. Long speleothem records have been produced from caves across Southeast Asia, but only a few samples approach annual resolution (e.g. Apipattanavis et al. 2009; Hu et al. 2008). With the exception of coral records covering a few centuries (e.g. Alibert and Kinsley 2008; Charles et al. 2003; Tudhope et al. 2001; Urban et al. 2000), the only natural proxy records with annual resolution from Southeast Asia are from tree rings. Most of the tree ring studies in Southeast Asia have involved three species from two countries, *Tectona grandis* (Buckley et al. 2007; D'Arrigo and Smerdon 2008; D'Arrigo et al. 2001, 2008, 2009; Pumijumnong et al. 1995), *Pinus merkusii* and *Pinus kesiya* (Buckley et al. 2005; Pumijumnong and

Eckstein 2011) from Thailand and Indonesia. *Tectona grandis* research now extends to Myanmar (D'Arrigo et al. 2011), and a few additional species have recently been added; *Pinus taiwanesis* in southeast China (Shi et al. 2010) and *Fokienia hodgensii* from Viet Nam (Buckley et al. 2010; Sano et al. 2009). The latter can sometimes exceed 1,000 years in age. *Tectona grandis* can also exceed 1,000 years, but almost all old teak was logged during the nineteenth and early twentieth centuries.

Some individuals of the species variant used in this study can also exceed 1,000 years. *Chamaecyparis obtusa* var. *formosana* [Hayata] Rehder 1914, hereafter *C.o.* var. *formosana*, closely related to the Japanese Hinoki [*Chamaecyparis obtusa* (Siebold et Zuccarini) Endlicher 1847], is native to the subtropical cloud forests of Taiwan. Trees in Taiwan's cloud forest band are immersed in clouds almost every day, especially in the afternoon (Chang et al. 2006). *C.o.* var. *formosana*, grows between 1,300 and 2,800 m in the mountains of northern and central Taiwan (Huang 1994), sometimes as a monospecific stand, but often intermixed with *Chamaecypris formosensis* (Matsum. 1901) and other species. Cloud immersion occurs on most days (Chang et al. 2006), but this species is strongly adapted to continued photosynthesis at medium to low light conditions (Lai et al. 2005). Highly prized for its lumber and fragrant oils, *C.o.* var. *formosana*, was heavily logged during the early and middle twentieth century. Samples for this study came from a large remnant of old growth forest.

Despite adequate water, relatively mild temperatures and a closed canopy, *C.o.* var. *formosana* tree rings show strong intercorrelation indicating a consistent common interannual climate influence. Climate data for temperature and precipitation amount were considered to identify the source of the common signal in these trees. Regression of the tree-ring time series on precipitation and temperature data revealed a significant relationship against NCEP/NCAR reanalysis I 700 hPa mean spring temperature (Kalnay et al. 1996; Kistler et al. 2001). Potential teleconnected relationships were investigated to identify climate features controlling temperatures in Taiwan's higher elevations. Significant correlations were identified from regressions of the tree-ring time series on spring values of two large scale climate indices, the East Asian Subtropical Jet Index (EAJI) and the Western Pacific pattern (WPI), but not with other potential teleconnections (e.g. East Asian Winter Monsoon). This study reports statistical indications of the local climate/tree-ring relationships and their teleconnections to the regional climate as represented by the EAJI and the WPI.

The East Asian Subtropical Jet is the dominant feature of the upper troposphere over the central North Pacific Ocean with a cool season core region over East China, the East China Sea, southern Korea and southern Japan, extending over the Northwest Pacific Basin (Park et al. 2010). First discovered in the 1920s as persistent cool season westerlies high above Tokyo, Japan (Lewis 2003), the position of the EAJ is now considered during trans-Pacific air travel as a cost-saving measure. The EAJ wind speed and jet trajectory are recognized as important influences on the North Pacific storm track (Chiang and Fang 2010; Lau 1988; Lee et al. 2010; Nakamura 1992; Wettstein and Wallace 2010), and links have been noted to trans-Pacific Asian dust transport (Gong et al. 2006, 2007), the East Asian Winter Monsoon (Jhun and Lee 2004) and East Asian spring drought (Park et al. 2010). An index of EAJ meridional activity (EAJI) based on 200 hPa wind speeds presents as a north–south dipole, with dipole changes interpretable as north–south latitudinal shifts in the EAJ core region (Park et al. 2010). The EAJ apparently fluctuates with ENSO-related changes through modification of the latitudinal extent of the Hadley Cell circulation. El Niño (La Niña) events have been associated with strengthening (weakening) of the Hadley Cell, and acceleration (deceleration) of the subtropical jets (Seager et al. 2003). The expectation under a global warming scenario is a poleward extension of the Hadley Cell, a consequence of increasing static stability in the troposphere, and a related strengthening of the EAJ along the poleward flank of the Hadley Cell (Lu et al. 2007).

Another important but less familiar feature of the upper atmosphere over the North Pacific is the Western Pacific pattern (WP), a 500 hPa geopotential height oscillation with poles that latitudinally bracket the higher EAJ core region. The WP was first isolated from atmospheric pressure data along with five other 500 hPa patterns (Wallace and Gutzler 1981) that include the more familiar Pacific North American pattern (PNA), and, after combining parts of two patterns, the North Atlantic Oscillation (NAO; Barnston and Livezey 1987). Wallace and Gutzler (1981) were the first to note links between the WP and fluctuations in the strength and position of the EAJ. Subsequent research has reported covariance of the WP phases with many climate features, including (1) zonal and meridional variation in the entrance region of the EAJ, in association with the position of the East Asian major trough (Gong et al. 2006), (2) downstream meridional changes in the location of the EAJ, especially in the exit region in the high latitudes of the eastern North Pacific (Linkin and Nigam 2008; Nigam et al. 2003), (3) baroclinic wave activity aloft north and downstream of the EAJ core region (Wettstein and Wallace 2010), and (4) pulsing of the North Pacific storm track intensity (Wettstein and Wallace 2010). The North Pacific storm track has also been linked to WP phases through changes in the number and character of Rossby wave breaking events; events that tend to reinforce the meridional shifts of the EAJ (Riviere 2010) and are recognized as important precursors to the high latitude blocking events that often modify storm tracks (Woollings et al. 2008). The cool season strength of the relationship between the EAJ and the WP is clearly

Table 1 Monthly correlation coefficients from the regression of the EAJ index on the WP index, 1958–2007

Jan	Feb	Mar	Apr	May	Jun
0.85*	**0.85***	**0.74***	**0.70***	**0.77***	**0.62***
Jul	Aug	Sep	Oct	Nov	Dec
0.21	0.15	0.19	0.36	0.48	**0.74***

Note the highly significant coefficients during the cool season and the rapid decrease after May (underlined and in bold). All values marked with '*' are significant at $p < 0.0001$

indicated by the highly significant correlation coefficients (Table 1) from monthly regressions of the EAJI (Park et al. 2010) on the WPI (Wallace and Gutzler 1981).

2 Materials and methods

2.1 Tree rings

Core samples of *C.o.* var. *formosana* were collected from northern Taiwan at 24.55N, 121.40E, between 1,900 and 2,060 m, using 5.1 mm diameter Haglöf increment borers. A minimum of two cores were collected per tree. After drying and mounting, the cores were sanded on the transverse surface, visually crossdated (Stokes and Smiley 1968) and measured to a resolution of 0.001 mm using a Velmex "TA" tree ring system. The crossdating was quality checked statistically using COFECHA (Holmes 1983).

Samples from more than one hundred trees were initially recovered. Inspection of these samples indicated that many *C.o.* var. *formosana* in the area suffer from extreme growth suppressions. Suppression-related problems often made cross-dating impossible for periods from many decades to centuries and sometimes required truncation or more commonly complete exclusion of the time series. Most of the ring-width time series that crossdated well over the entire length of the samples came from trees growing in a southwest-trending valley located immediately below and to the southwest of a major northwest-southeast-trending ridge. The valley was also bordered by low ridge lines to the northwest and southeast. Trees growing in locations outside of the valley were often missing their tops or major limbs, were often rotten or hollow, and often had severe growth suppressions. These features were much less frequent within the valley suggesting that the topography has provided protection from storm damage.

Ring width time series from fifty cores, representing thirty trees, were used to produce a mean ring width chronology (CIL STD). The tree ring width measurements were standardized following accepted methods. The data were first power transformed, to reduce end effects and heteroskedasticity in the variance, and to allow the use of residuals during indexing (Cook and Peters 1997). The data were then detrended using a 100-year cubic spline (Cook and Peters 1981), and indexed using the residuals (Cook and Peters 1997). Tukey's biweight robust mean was used to combine the series as suggested by Cook (1985) for closed canopy forests. A robust autocorrelation model was chosen to control for outliers. The mean series length for the 50 time series was 605 years, with a mean intercorrelation of $r = 0.55$. The Expressed Population Signal (EPS) was calculated from the tree mean time series to determine the years over which the mean chronology common signal exceeds the accepted proportion (0.85) of the signal in a theoretically infinite population (Wigley et al. 1984).

2.2 Climate

Climate/tree-ring relationships were investigated using precipitation and temperature data from many sources, including gridded climate data from the Climate Research Unit (CRU TS3.1; Mitchell and Jones 2005), NCEP/NCAR Reanalysis I data (NNR; Kalnay et al. 1996; Kistler et al. 2001), and data from local meteorological stations. Indices for climate features potentially important to the climate of Taiwan were also considered; including an index of the Western Pacific pattern (WPI) obtained from the Climate Prediction Center of the National Oceanic and Atmospheric Administration (http://www.cpc.noaa.gov), an index of the East Asian Subtropical Jet Stream (EAJI) produced using NNR 200 hPa zonal wind data following Park et al. (2010), and an index of the East Asian Winter Monsoon (EAWMI), produced using NNR 300 hPa zonal wind data following Jhun and Lee (2004). The WPI, a dipole of 500 hPa pressure heights identified by rotated principal component analysis, manifests as two centers of actions, one over the Kamchatka peninsula, and another over parts of Southeast Asia and the western subtropical North Pacific. The EAJI was defined by Park et al. (2010) as the "area-mean difference [U200 (40°N–51°N, 120°E–180°E)] minus [U200 (21°N–32°N, 110°E–170°E)] of the composite of spring zonal wind speed anomalies", with the intention of identifying meridional shifts in the position of the EAJ core region. Positive (negative) deviations in the EAJI indicate a northward (southward) displacement of the EAJ core. EAWMI was defined by Jhun and Lee (2004) as the "difference in the area-averaged zonal wind speed at the 300-hPa level", U_{300}(27.5°–37.5°N, 110°–170°E) − U_{300}(50°–60°N, 80°–140°E). All spatial correlation analyses presented in this paper were performed on the Koninklijk Nederlands Meteorologisch Instituut (KNMI) Climate Explorer website (http://climexp.knmi.nl).

The analyses for this study start with the first International Geophysical Year, 1958, to ensure the reliability of

the upper air data (Grant et al. 2009; Kistler et al. 2001). One problem with Radiosonde and Rawinsonde (RAOB) data collected prior to 1958 is inhomogeneity of the resulting data and nonstandard launch times (Grant et al. 2009). Pibal (pilot balloon) wind speed data are available for many locations prior to 1958, but pressure and temperature measurements were not recorded until the beginning of RAOB measurements. Inadequate spatial coverage of the available data is another problem, especially for studies involving teleconnections, because mathematically accurate upper air data can still yield poor correlation coefficients in teleconnected regressions if insufficient numbers of data points are available for precise estimation of values for the non-measured locations. Data coverage is good back to 1957 over the western part of a region bounded by 110E–180E and 20N–50N, an area that includes Taiwan, Eastern China, Korea, Japan, and a large area of the western North Pacific, but the coverage drops quickly prior to that year (Online Resource). The boundaries of the region specified in the previous sentence were chosen based on the coordinates used to define the EAJI (Park et al. 2010), a climate index used in this study.

Significant common frequencies between the tree rings and climate time series were determined using a multitaper version of magnitude squared spectral coherence (Mann and Lee 1996). Spectral coherence is the square of the absolute cross-spectral density of the two time series divided by the product of their autospectral densities; the correlation between the two time series in the frequency domain. The use of multiple tapers minimizes spectral leakage and thus provides a better balance between spectral resolution and statistical variance than single-taper methods (Thomson 1982). We used three 2π tapers and a red noise background null hypothesis as recommended for instrumental climate records (Ghil et al. 2002). Common significant frequencies between the tree ring and climate time series were only identified in the higher frequencies, so frequency filtering was investigated to enhance the climate signal.

High-pass filtering of the CIL STD chronology was really the second high-pass filter applied to the tree ring data, because detrending of the individual tree-ring time series, a standard dendroclimatological technique (e.g. Cook et al. 1990), requires the use of a high pass filter. The filtering techniques considered for the second high pass filter were Box filtering (moving average), Binomial filtering and LOESS filtering (Cleveland and Devlin 1988). The three filtering techniques use very different taper functions (window functions): (1) Box filtering equally weights all data points within the chosen window size, (2) Binomial filtering uses a symmetrical window produced by weighting the data points within each window based on a quasi-Gaussian distribution whose characteristics are determined by the window size (the number of weights), and (3) LOESS filtering uses weighting of the data points within each window based on weighted least squares fitting of a polynomial curve to the data points, so the result is usually non-symmetrical. Each low-pass filter was applied to the original tree-ring and temperature time series using frequency cutoff values chosen so as to *exclude* the frequency range identified in the spectral coherence analysis, thereby *including* the range after the low-pass version was subtracted from the original data (High pass filters are usually produced by differencing a low pass filtered time series from the original time series). Using a short window with a LOESS filter can cause errors and allow outliers to affect the output (Cleveland and Devlin 1988), but the previous application of the Tukey biweight robust mean during detrending and the use of a robust method for the modeling of autocorrelation during chronology generation controls for outliers, thereby ensuring that input data is appropriate for LOESS filtering. Regression results for all three filtering methods, using window sizes of 2–6 years, and a short discussion, are presented in Online Resource Table 1. A 5-year LOESS filter was chosen for all subsequent analyses.

Climate parameters were reconstructed from LOESS high-pass filtered versions of the tree-mean tree-ring and climate data using a split period procedure (Meko and Graybill 1995), where one continuous portion of the data is used to calibrate, and the other continuous portion is used to validate. Reduction of error (RE) and coefficient of efficiency (CE) statistics (Cook et al. 1990) were used to evaluate the skill of the reconstruction model. RE and CE values that exceed zero indicate model skill (Cook et al. 1999), with a maximum value for both RE and CE of one. A Generalized Least Squares (GLS) approach was applied during the reconstruction to account for the influence of autocorrelation of the time series (Pinheiro and Bates 2000).

Time series of multiple covarying climate parameters may all have statistically significant relationships in regressions on a single tree-ring time series, and reconstructions based on simple linear regression relationships from ordinary least squares (OLS) analysis are linear transfer functions, so multiple predictands may sometimes be reconstructable from the same predictor (the tree-ring time series). A generalized least squares (GLS) approach (Pinheiro and Bates 2000), or similar, is required when either autocorrelation is significant or variance is heteroskedastic. In GLS, heteroskedasticity and autocorrelation are removed by linear transformation of the data based on an autoregressive model prior to OLS transformation. If the reconstruction is based on a linear relationship, and the same autocorrelation model is used for all the reconstructions, then the reconstructions will differ only by a scaling factor and error terms, and a regression of the reconstructions on each other will have a correlation coefficient of $r = 1.0$.

3 Results

No significant correlations were identified between the CIL standard (CIL STD) chronology and temperature (or precipitation) from surface gridded climate data (CRU TS3.1) or from local meteorological stations, including lagged relationships. Similarly, no significant correlations were identified for the year of tree ring formation in regressions on NCEP/NCAR reanalysis I data (NNR; Kalnay et al. 1996; Kistler et al. 2001). However, significant correlations were found against NNR climate data when the CIL STD chronology was lagged by 1 year (t^{-1}) and regressed on March–May NNR lower troposphere mean temperatures over Taiwan (21–26N 119–121E). Regression of the lagged CIL STD chronology on mean temperature values at 700 hPa (March–May NNR 700 hPa T) were the most significant, ($r = -0.37$, $N = 50$, $p < 0.03$).

Exploration of CIL STD t^{-1} regressions on regional climate indices revealed significance against the March–May means of the EAJI and WPI climate indices (EAJI, $r = -0.37$, $N = 50$, $p < 0.05$; WPI, $r = -0.43$, $N = 50$, $p < 0.01$). Support for the importance of these relationships to CIL tree growth was suggested by significant correlation coefficients from regressions of the March–May means of both the EAJI and the WPI on the March–May NNR 700 hPa T time series, at t^0. No significant correlations were found between the CIL STD chronology and the East Asian Winter Monsoon index (EAWMI).

Multiple taper spectral analysis of the CIL STD chronology indicated significance at many frequencies between 2.0 and >128 years (not shown), but analysis of the March–May 700 hPa T data indicated significant frequencies only between 2.5 and 4.0 years (not shown), the same frequencies indicated by multiple taper spectral coherence analysis comparing the CIL STD and the March–May NNR 700 hPa T time series (Fig. 1). Significant peaks in the same 2.5–4.0 year range were revealed by multiple taper spectral coherence comparisons of the March–May means of the WPI and the NNR 700 hPa T and the March–May means of the EAJI time series and the NNR 700 hPa T (Fig. 1).

Three methods of high pass frequency filtering were tested by applying them to the CIL STD, March–May EAJI and March–May WPI, and March–May 700 hPa T time series, regressing the first three separately on the March–May 700 hPa T time series, and then assessing the significance of the resulting correlation coefficients. All the results were highly significant, though the significance of the LOESS filtering consistently exceeded that of the other methods (see Online Resource). A 5-year LOESS filter was chosen from among the possible LOESS window sizes so as to include the significant frequencies previously identified by multiple taper singular spectral and spectral coherence analyses (Fig. 1). A 5-year LOESS filter was used in all subsequent analyses. Regression results from before and after frequency filtering are presented in Table 2. High pass filtering of the EAWMI (EAWMI 5YR) did result in a marginally significant relationship from regression of March–May EAWMI 5YR on the CIL STD 5YR chronology ($r = 0.29$, $p < 0.05$), but the relationship explained little of the variance, so no further analyses were done. The acronyms for the resulting 5-year LOESS filtered time series are CIL STD 5YR, WPI 5YR, EAJI 5YR and March–May NNR TMn 700 hPa 5YR.

Figure 2 presents spatial correlation maps from regressions of the March–May NNR TMn 700 hPa time series

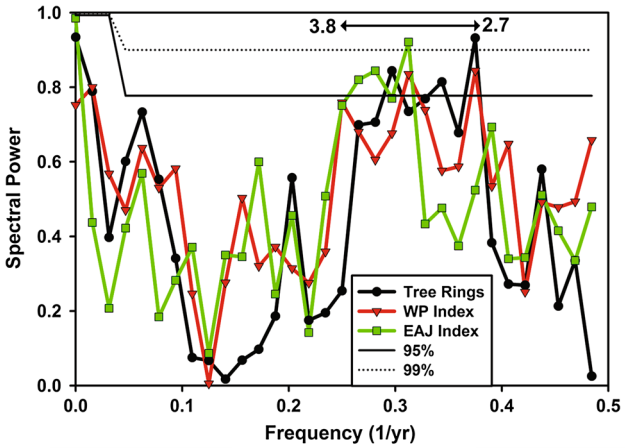

Fig. 1 Multiple taper spectral coherence analysis up to 5 years for the CIL tree-ring chronology, the East Asian Jet Index (EAJI), and the Western Pacific Pattern index (WPI) against the March–May 700 hPa mean temperature over Taiwan. The *horizontal solid and dotted lines* indicated the 95 and 99 % significance levels

Table 2 Correlation coefficients from the regression of the CIL tree ring chronology, at lag 1, on March–May mean values for 700 hPa temperature over northern Taiwan, the EAJ index (EAJI) and the WP index (WPI). Correlation coefficients from regressions of two high pass time series are highlighted

	Tmn	Tmn 5YR
CIL STD	−0.37*	−0.39*
CIL STD 5YR	−0.51****	**−0.57****
	WPI index	WPI 5YR
CIL STD	−0.39**	−0.42**
CIL STD 5YR	−0.56****	**−0.63****
	EAJI index	EAJI 5YR
CIL STD	−0.32*	−0.37*
CIL STD 5YR	−0.48***	**−0.56****

The regressions were performed on the original data and on 5-year high pass versions of each dataset. $p < 0.05$ = *, <0.01 = **, <0.005 = ***, <0.001 = ****. $N = 50$ for the original datasets and $N = 49$ for the LOESS filtered datasets

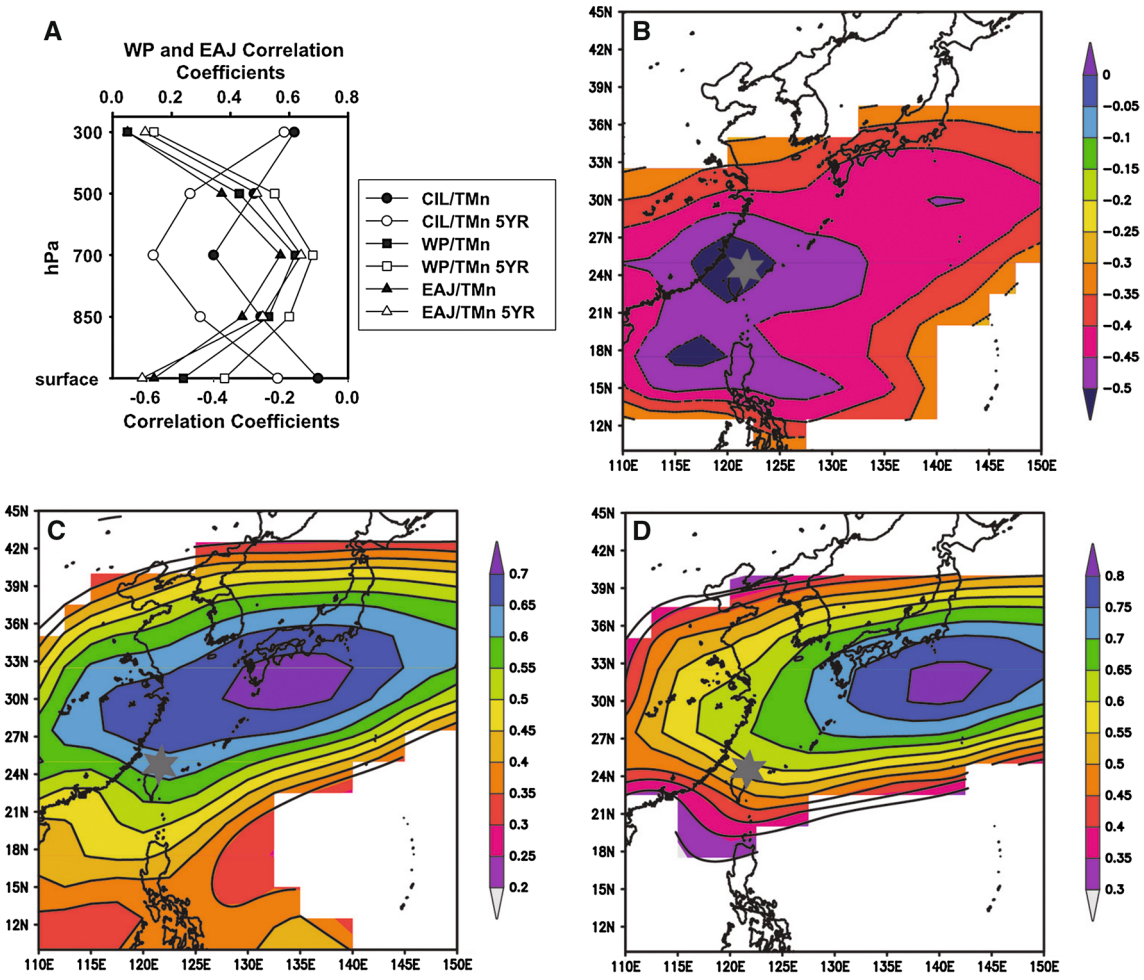

Fig. 2 **a** Correlation coefficients from regression of CIL STD, CIL STD 5YR, March–May WPI, March–May WPI 5YI, March–May EAJI, and March–May EAJI 5YR on NNR March–May mean temperature over northern Taiwan at standard pressure levels, **b** spatial correlations from regressions of CIL STD 5YR on 700 hPa NNR March–May mean temperature, **c** spatial correlations from regressions of the March–May mean WP index on 700 hPa NNR March–May mean temperature, and **d** spatial correlations from regressions of the March–May mean EAJ index on 700 hPa NNR March–May mean temperature. The *white circle* and *white triangle* refer to values for regressions of the temperature data on CIL standard and CIL STD 5YR tree-ring chronologies, respectively. The *black circle* and *black triangle* refer to values for regressions of the temperature data on STD and LOESS 5YR, respectively. The *black star* indicates the location of the tree site

on the CIL STD 5YR time series (Fig. 2b), on the March–May WPI 5YR (Fig. 2c) and on the March–May EAJI 5YR (Fig. 2d) over a grid covering 10N–45N and 110E–150E. The correlations of the 5-year LOESS filtered time series, CIL STD 5YR, March–May EAJI 5YR and March–May WPI 5YR, against the March–May 700 hPa T were most significant at 700 hPa, extending over a large region, especially in regressions on the March–May EAJI 5YR and March–May WPI 5YR time series. The correlation coefficients decreased above 700 hPa and toward the surface (sea level), and were not significant at the surface against the tree rings or the climate indices (Fig. 2a). One surface parameter from the CRU TS3.1 gridded time series did show significant correlation against the CIL STD 5YR chronology after high-pass LOESS filtering, Feb–May mean vapour pressure (Online Resource). We hypothesize that changes in both high elevation temperature and water vapour affect the cloud height/density at the tree site.

March to May average values for WPI 5YR and EAJI 5YR for A.D. 1000–2007 were reconstructed based on regressions against the CIL STD 5YR time series (Fig. 3). A Durbin–Watson test indicated the data modeled as an AR3 process, so the GLS method (Pinheiro and Bates 2000) was applied. A split period calibration/verification procedure (Meko and Graybill 1995) was used to test the stability of the regression model. Both periods passed a Shapiro–Wilk test of normality. Reduction of error (RE) and coefficient of efficiency (CE) statistics were positive in all cases (Table 3), indicating model skill (Cook et al. 1999). The GLS reconstruction models for WPI 5YR and EAJI 5YR explained

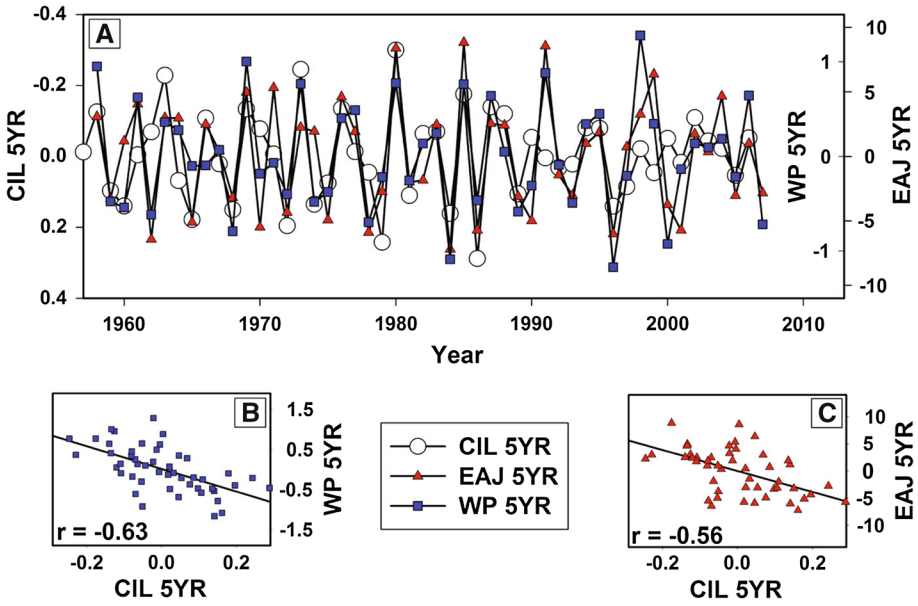

Fig. 3 **a** Plot of the Mar–May means of CIL STD 5YR, WPI 5YR and EAJI 5YR (the tree ring *y*-axis, CIL 5YR, is inverted); **b** regression of CIL STD 5YR on Mar–May mean WPI 5YR, at lag 1; **c** regression of CIL STD 5YR on Mar–May mean EAJI 5YR, at lag 1. CIL STD 5YR values are presented as *circles*. WPI 5YR values are presented as *squares*. EAJI 5YR values are presented as *triangles*

Table 3 Statistics from reconstruction of the March–May WPI 5YR and EAJI 5YR using a split period calibration/verification

Period	Calibration			Period	Verification		
	r	r^2	RMSE		*r*	RE	CE
Mar–May WPI 5YR reconstructed from CIL 5YR							
1958–1982 (1st half)	−0.67****			1983–2006 (2nd half)	−0.65****	0.52	0.44
1983–2006 (2nd half)	−0.65****			1958–1982 (1st half)	−0.67****	0.18	0.29
1958–2006 (full period)	−0.66****	0.39	0.49				
Mar–May EAJI 5YR reconstructed from CIL 5YR							
1958–1982 (1st half)	−0.53**			1983–2006 (2nd half)	−0.59***	0.30	0.28
1983–2006 (2nd half)	−0.59***			1958–1982 (1st half)	−0.53**	0.14	0.17
1958–2006 (full period)	−0.55***	0.30	3.9				

Significance: $p < 0.05$ = *, <0.01 = **, <0.005 = ***, <0.001 = ****; *r* = Pearson correlation coefficient; r^2 = coefficient of determination; RE = reduction of error; CE = coefficient of efficiency. RE and/or CE > 0.0 shows skill in the model reconstruction. RMSE = root mean squared error. The correlation coefficients (*r*) presented were corrected for autocorrelation as an AR3 process (Dawdy and Matalas 1964). The coefficients of determination (r^2) presented are based on simple linear regression of the observed values on the generalized least squares predicted time series. Reconstruction using generalized least squares instead of ordinary least squares reduced the variance explained by about 2 %

39 % and 30 % of the variance, respectively. Reconstructed WPI and EAJI are presented in Fig. 4. A positive trend in the running variance after the middle nineteenth century is significant based on results of a modified Mann–Kendall test designed to account for autocorrelation (Hamed and Rao 1998; Yue and Wang 2004).

4 Discussion

4.1 Tree physiology and climate: lagged relationships

Recovery of dendroclimatological information from the closed canopy cloud forests of Taiwan required the use of techniques that are not typically applied in most dendroclimatological research, including fairly extreme high pass filtering of the time series, recognition of a climate influence on tree growth only as a lagged relationship and application of generalized least squares during the reconstruction, to account for significant autocorrelation. The aforesaid relationships were recognized during the dendroclimatological evaluation of a 1,093-year ring width chronology developed from *Chamaecyparis obtusa* var. *formosana* (*C. o.* v. *formosana*), a tree species native to the mountains of northern Taiwan. Taiwan cloud forests are immersed in fog on most days, especially in the afternoon (Mildenberger et al. 2009), a phenomenon caused by the uplift of moist lowland air by orographic and valley winds. Available sunlight is

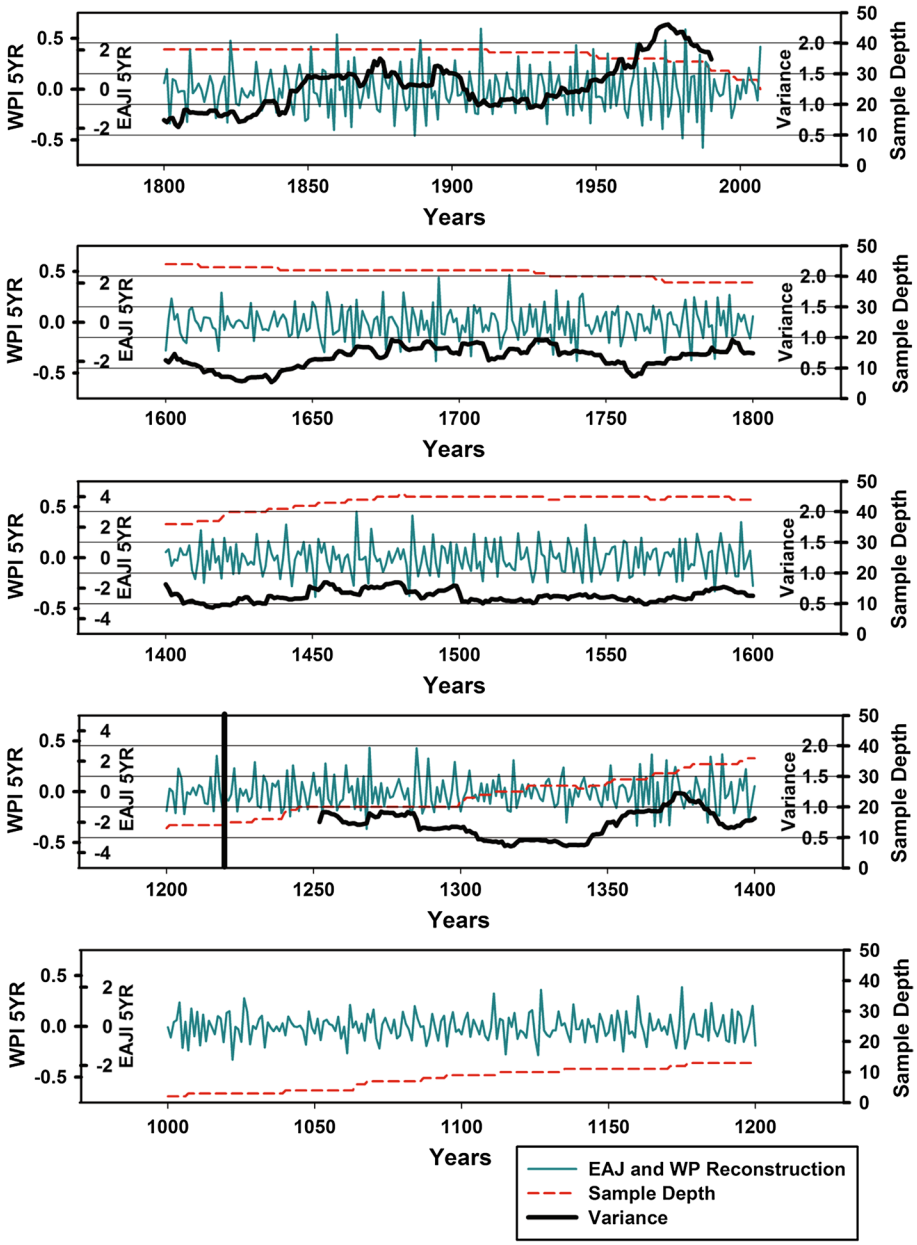

Fig. 4 Reconstruction of March–May mean WPI 5YR and March–May mean EAJ I 5YR. Sample depth is indicated by the *stepped dashed line*. Variance as a running 33-year mean is indicated by the *solid black line*, with the datapoint being the middle year of the 33-year window, and is scaled for the EAJI reconstruction. The *thick vertical line* indicates the year when the Expressed Population Signal drops below 0.85

greatly reduced when the fog forms (Lai et al. 2006), so tree species within the cloud forest zone must be able to photosynthesize under low light conditions. *C. o.* v. *formosana*, the study species, is particularly well adapted in this regard (Lai et al. 2005).

Despite the low-light growing conditions experienced by *C. o.* v. *formosana*, the ring width time series sampled in this study show significant intercorrelation, indicating sensitivity to climate changes. Yet initial regressions of a standard ring width chronology of *C. o.* v. *formosana* (CIL STD) against precipitation and temperature from Taiwan meteorological station data and gridded surface climate data (CRU TS3.1; Mitchell and Jones 2005) revealed no significant relationships. Regressions on NCEP NCAR Reanalysis 1 (NNR; Kistler et al. 2001) temperature and precipitation data at all standard pressure heights from the surface to 200 hPa also failed to show significance against the current growing season, so lagged relationships to climate were considered.

Significant correlations were identified in regressions of the CIL STD chronology against March–May NNR mean temperature in the middle and lower troposphere over Taiwan at a lag of 1 year, especially at 700 hPa ($r = -0.38$, $p < 0.01$), the closest standard pressure level above the tree site (Fig. 2a). Also significant at a lag of 1 year were regressions of the CIL STD chronology on the March–May mean of indices of the Western Pacific pattern (WPI; $r = -0.39$, $p < 0.01$) and the East Asian Subtropical Jet (EAJI;

$r = -0.32$, $p < 0.05$), which were in turn significantly correlated with the same 700 hPa March–May NNR mean temperature over Taiwan (Fig. 2c, d). While significant, the relationships between the CIL STD chronology and the climate parameters did not explain much of the variance.

Many researchers have proposed that variations in incident radiation are the most important factor controlling photosynthesis in cloud forests (Bruijnzeel and Veneklaas 1998; Letts and Mulligan 2005; Mildenberger et al. 2009; Chu et al. 2014), and the results from this study are consistent with the radiation limitation hypothesis. *C.o.* var. *formosana* is well adapted to continued photosynthesis under even low light conditions (Lai et al. 2005), but various measures indicate that maximum photosynthetic activity of *C.o.* var. *formosana* occurs under medium light conditions (Lai et al. 2005). We propose that the temperature-related growth changes in the study trees are caused by changes in available sunlight via temperature-mediated changes in the amount of cloud and/or the height of cloud formation.

Lagged relationships to climate are common in tree-ring analyses, and usually involve the use of stored photoassimilates during the current growing season and/or developmental processes (e.g. leaf maturation, root elongation) in the previous growing season (Fritts 1976). Yet a climate/tree-growth relationship manifested only as a lagged relationship is unusual. The most likely physiological link between temperature in the prior Spring and wood formation the following year is differences in the photosynthetic capacity of developing leaves, caused by variations in the incident radiation, equivalent in many ways to the recognized physiological differences between sun and shade leaves (Valladares and Niinemets 2008). Leaves are phenotypically plastic for some traits, even in shade tolerant species (Valladares and Niinemets 2008), and while biochemical changes related to photosynthetic capacity may acclimatize during the year, some anatomical changes, such as leaf size and mesophyll structure, may be irreversible (Ishii 2011; Wyka et al. 2008). The source of photoassimilates contributing to xylem production in the beginning of the growing season is storage and new production from mature leaves, not new growth, so a change in the photosynthetic capacity of the earliest growth in leaves produced in one year will have a greater influence on net carbon export in the following year, and consequently on xylem production in that year. Another contributing factor may be the leaf dimorphism (e.g. juvenile-adult) that is characteristic of almost all members of *Cupressoideae* (Farjon 2010). The study species, *Chamaecyparis obtusa*, retains 4–6 years of foliage (Miyamoto et al. 2013), so the postulated relationship between available radiation and leaf anatomy could be tested for this site by measuring pertinent leaf characteristics of early growing season tissue from the 4–6 years of leaves retained and comparing them with measurements of mean March–May radiation as recorded at the flux tower of an LTER site established in 2002 within 15 km of the study site (Chang et al. 2006).

4.2 Tree physiology and climate: high frequency relationships

Magnitude-squared spectral coherence analysis was applied to determine the important common frequencies in both the climate and tree-ring time series. A multiple taper spectral coherence comparison (Mann and Lee 1996) of the CIL STD chronology and March–May 700 hPa TMn revealed significant common frequencies between about 2.5 and 4.0 years (Fig. 1). The existence of significant shared peaks only in the higher frequencies suggested that high-pass filtering of the datasets would increase the significance of the tree-ring width/climate relationship. Results from tests of different methods for producing high pass filters indicated a 4 or 5 year high pass LOESS filter as consistently the best choice for windows of 4, 5 and 6 years, though results from Box filtering and Binomial filtering were almost as significant (Online Resource). High-pass filtered versions of the CIL STD chronology (CIL STD 5YR), the WPI and EAJI (EAJI 5YR and WPI 5YR) and the NNR 700 hPa TMn over Taiwan were produced using the 5-year LOESS filter. Regressions of the high frequency versions of the climate indices on the CIL STD 5YR chronology resulted in large increases in the significance of the correlation coefficients (Table 2), with the means of March–May remaining the most significant. CIL STD 5YR, EAJI 5YR, and WPI 5YR are plotted in Fig. 3, as time series for ease of comparison, and as regressions of CIL STD 5YR on each of the high pass filtered climate indices.

A tree-ring width climate signal manifested almost entirely in the higher frequencies is consistent with the influence of closed canopy forest dynamics on tree-ring formation. Tree-ring widths in closed canopy forests tend to be dominated by local medium-frequency non-climate influences such as competition, gap dynamics, insect outbreaks and pathogens (e.g. Fritts 1976; Phipps 1982; Berryman et al. 1987, Ise and Moorcroft 2008), not by climate. Gap dynamics are particularly important in Taiwan's cloud forests. Common occurrences are uprooting and major damage to the photosynthetic and water transport apparatus (e.g. loss of the top or major branches) caused by the high-speed winds that accompany the 3–4 typhoons that affect Taiwan's weather annually. Uprooting and major damage, such as missing tops or major branches, are common occurrences whose effects can last for many decades.

4.3 Reconstructed climate indices and long-term trends

Both EAJI 5YR and WPI 5YR were reconstructed for A.D. 1000–2007 using relationships identified from simple

linear regressions on the CIL STD 5YR chronology, following generalized least squares modifications to account for an autocorrelation-related lack of independence in the errors (Table 3; Fig. 4). The reconstructions can be overlain exactly following careful scaling, because the reconstructions are linear transformations of the CIL STD 5YR chronology with autoregressive modeling of the same order for both reconstructions. Certainly the WPI 5YR and EAJI 5YR time series are not identical, but regression of the March–May mean WPI 5YR on the March–May mean EAJI 5YR explains over 60 % of the variance ($r = 0.78$, $N = 49$), and it is a large portion of this shared variance that is being captured by the linear transformation of the CIL STD 5YR time series. The difference between the reconstructions lies in the amount of variance explained by the regressions (Table 3), and therefore in the accuracy of each reconstruction.

Both the climate indices were produced from data covering very large regions above the North Pacific, but conceivably the common pattern between the tree rings and the climate indices could be dominated by the portion of the region closest to Taiwan. To test this idea, we compared the March–May 200 hPa wind speed anomalies during the twenty extreme ring-width years in the common period, 1958–2007, ten large ring years and ten small ring years, at a lag of 1 year (Fig. 5b). The difference in the 200 hPa wind speed between these groups of years is greatest over the central North Pacific. Higher (lower) velocity zonal winds to the north of the EAJ core region over the eastern North Pacific preceed smaller (larger) extreme growth years in the CIL STD 5YR chronology. The converse is true to the south of the EAJ core region. The latitudinal position of the EAJ over the land/ocean transition north of Taiwan is relatively stable seasonally (Fig. 5a), so the differences noted over the central North Pacific correspond to a more meridional (more zonal) flow in the EAJ in the years prior to smaller (larger) CIL STD 5YR ring widths.

Perhaps of more interest climatologically than high frequency reconstructions of these climate indices is the strong upward trend in their variance after about A.D. 1850, presented here as 33-year running mean values plotted on the final year of the 33-year windows (Fig. 4). A Mann–Kendall test of trend, modified to correct for autocorrelation (Hamed and Rao 1998; Yue and Wang 2004), indicates that the trend in the running variance is significant. Despite the significant result from the Mann–Kendall test, the trend is not monotonic, with clear peaks in the late-nineteenth and late-twentieth centuries. A slight reduction in the variance is noted after about 1975, but the values after 1975 still exceed any values prior to about 1960. This recent downward trend in running variance the CIL STD 5YR is matched by similar downward trends in the WPI 5YR and EAJI 5YR time series (Online Resource).

Support for existence of a long-term upward trend in the EAJ seems to be provided by Moore (2013) who reports instrumental and ice core evidence for a trend in the strength of the EAJ beginning by 1871. His analysis compared snow accumulation and dust concentration from the Tibetan Plateau with wind speed data from the NNR (Kalnay et al. 1996; Kistler et al. 2001) and as estimated from surface pressure data in the much longer twentieth century reanalysis (20CR; Compo et al. 2011). Moore (2013) also reports a recent reduction in the EAJ index, specified as starting in about A.D. 2000, though arguably the reduction may begin when Moore's wind speed index flattens in around 1980 (Figure 3A in Moore 2013). The latter timing would be temporally consistent with the reduction in variance noted in our study. While the months used to construct the EAJSI indices in Moore (2013) are not specified, they certainly included the core months for the EAJ, December–February, perhaps suggesting that the long-term trend we note in the EAJ variance is not limited to March–May.

Moore's index, calculated as the spatial mean of 200 hPa wind speeds, includes all of the region between the two poles of the index defined by Park et al. (2010) to bracket the EAJ core region, and most of the region used to produce the Park et al. (2010) index dipoles themselves, EAJI in this paper. Consequently, the Moore (2013) index cannot identify latitudinal shifts in the EAJ. Use of the 20CR dataset by Moore (2013) to identify long-term changes in the EAJ wind speed seems appropriate, but the spatial inaccuracy introduced by reliance on surface data to estimate upper air data values and the rapid decrease in the density of datapoints before about 1950 (Online Resource) preclude the use of the 20CR in the current study, where upper air spatial changes need to be accurately identified and quantified. Evidence of the reduced accuracy of the 20CR is clear in results of a simple linear regression comparison for the common period (1948–2010) of EASJI indices produced using both NNR and 20CR data (Moore 2013). Despite being estimates of the same parameter, the correlation coefficient from the regression of 20CR on NNR explains only 50 % of the variance (Moore 2013).

4.4 Interpretation

The CIL STD 5YR chronology only provides point source information about the changes in the EAJ and WP indices, so interpretations in terms of atmospheric dynamics are necessarily suspect, and perhaps analogous to the old story from India where descriptions of an elephant vary tremendously among a group of blind men who individually feel only one part. What does a strong trend in the long-term variance in the EAJI 5YR and WPI 5YR indicate? For the EAJI, does the trend in variance indicate long-term changes in the EAJ core wind speed or latitudinal shifts, or both?

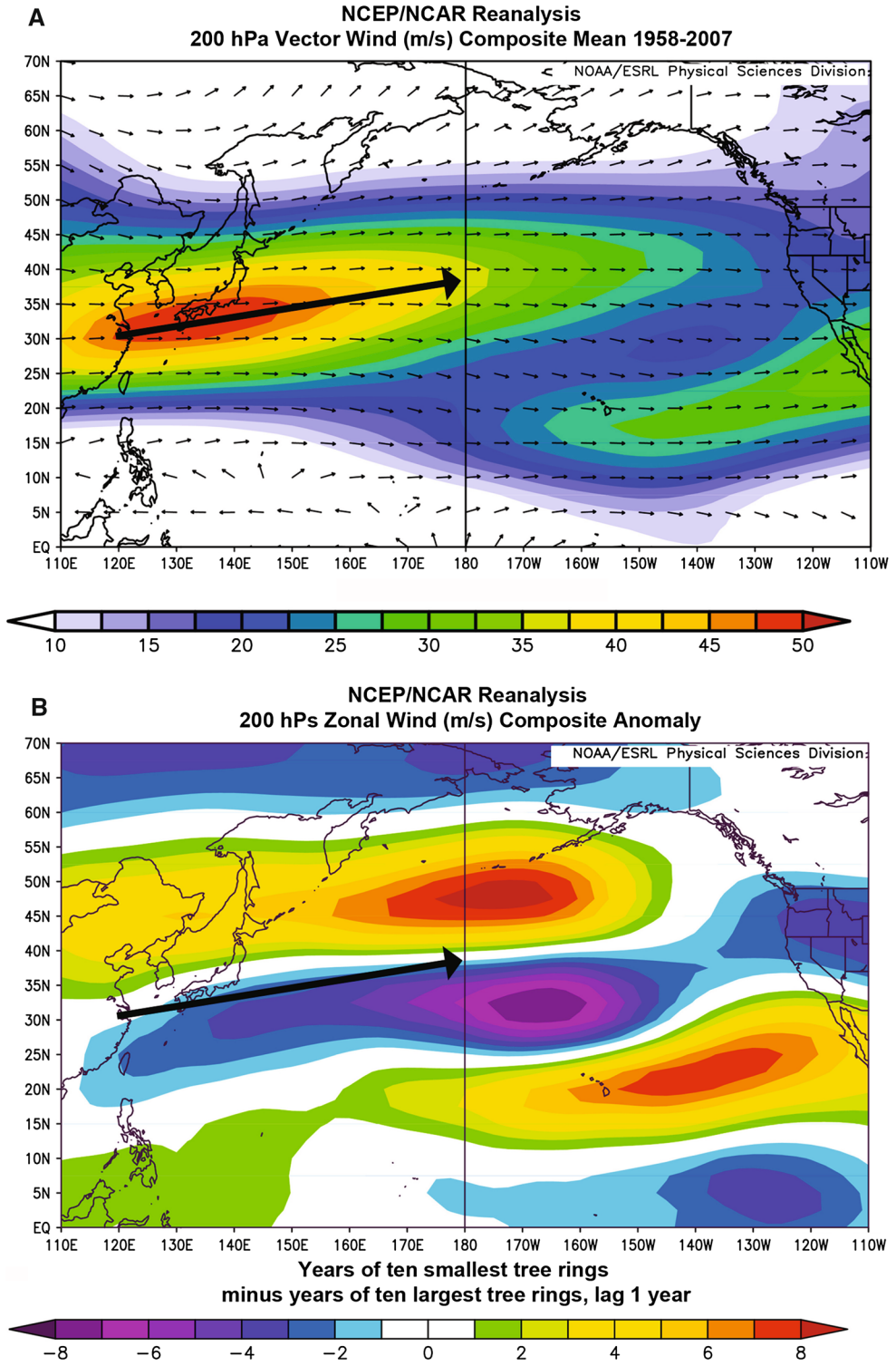

Fig. 5 200 hPa vector winds over the northern Pacific. **a** The March–May composite mean vector wind speed and direction for the period of tree-ring comparison, 1958–2007. **b** The March–May zonal wind speed and direction anomalies as the difference between the ten smallest tree-ring years and the ten largest tree-ring years. The *black arrows* approximate the mean location of the EAJ core. Modified from an image provided by the NOAA/ESRL Physical Sciences Division, Boulder Colorado from their Web site at http://www.esrl.noaa.gov/psd/

Is the long-term shift identified from a Taiwanese vantage point only regionally applicable, or indicative of changes in hemispheric or global circulation?

Evidence that the long-term trend in variance of the reconstructed EAJI should be interpreted as a shift in the mean position of the EAJ core relative to Taiwan, not as long-term changes in the amplitude of inter-seasonal shifts in a latitudinally stable EAJ, is suggested by recent research investigating the influence of global warming on the Hadley Cell and on the subtropical jets (Seager et al. 2003, 2005; Lu et al. 2007). Results of this research indicate that changes in the El Niño-Southern Oscillation drive changes in Hadley Cell dimensions (Seager et al. 2003, 2005; Lu et al. 2007). El Niño (La Niña) events coincide with strengthening (weakening) of the Hadley Cell, equatorward (poleward) movement of the Intertropical Convergence Zone and strengthening (weakening) of the subtropical jets (Seager et al. 2003, 2005). Equatorward strengthening of the subtropical jets is associated with eastward extension of the Pacific storm track through increased longevity of baroclinic eddies (Seager et al. 2005). An upward trend in the latitudinal breadth of the Tropical Belt starting around 1979 has already been identified (e.g. Seidel et al. 2008), timing that is coincident with the apparent recent downturn in the EAJ (and WPI) variance as identified in this research (Fig. 4 and Online Resource). The coincident timing may indicate that the recent reduction in variance in the Taiwan tree ring widths has been caused by a poleward shift in the EAJ, reducing the influence on the tree rings by increasing the distance. Yet this interpretation seems inconsistent with the longer-term shift in the variance which began in the middle of the nineteenth century. If the downward trend in variance in recent years was caused by poleward movement of the EAJ core region, then the much lower variance in the tree-ring widths during the pre-instrumental period would seem to indicate a more poleward position of the EAJ prior to A.D. 1850.

Another possibility exists. Changes in the proximity of trees to a spatially fluctuating influence on tree growth (e.g. EAJ and WP), whether the fluctuations are in intensity, in mean location, or both, will not necessarily have a linear influence on the tree-ring growth. At some large distance from the Taiwan tree site, influence of the EAJ/WP on the ring width variance would be nonexistent, so there would be no meaningful direct statistical relationship between time series of the EAJ/WP and the Taiwan tree growth. At very close proximity to the Taiwan tree site, the effect of the EAJ/WP on Taiwan tree growth may be almost constant, because a growth factor must vary to be identified statistically. Consequently, lower variance in the CIL STD 5YR chronology prior to the mid-nineteenth century could indicate that the EAJ core was closer to or even directly over Taiwan.

How can these hypotheses be tested? Regressions of EAJI 5YR on mid-troposphere temperature (e.g. NNR 700 hPa TMn 5YR) are highly significant over south and central Japan during the northern hemisphere spring (Fig. 2c, d), so one potential source of additional information about EAJ variance is counterpart tree sites growing under similar conditions in Japan. Japanese high elevation tree sites exist for the same species, *Chamaecyparis obtusa*, and for other high elevation Japanese tree genera such as *Tsuga*, *Picea*, *Abies* and *Cryptomeria*. An upward trend in the high frequency ring width variance of trees growing in Japan north of the spring EAJ position, the same trend as the Taiwanese trees, and therefore on both sides of the EAJ, would indicate a long-term change in the strength/breadth of the EAJ/WP at a relatively constant latitude. Trends of opposing sign on opposite sides of the EAJ would indicate a long-term latitudinal trend in the spring EAJ/WP core region. Yet biology may limit such a comparison, because environmental differences related to latitude (e.g. temperature, light angle) are among the factors that determine tree phenology, so the timing of a teleconnection between the EAJ/WP and Japanese trees may differ from the months noted for northern Taiwan.

4.5 Asian dust transport

Another potential effect of changing variance in the EAJI and the WPI is changes in the loading, transport and deposition of Asian dust, particularly in transport to the eastern North Pacific and North American continent (Gong et al. 2006). Gong et al. (2006) specify differences in dust loading in the desert regions of East Asia as being related to changes in the meridional wind speed. Stronger wind speeds close to the deserts are caused by a shift in the mean position of the westerly trough to closer to the desert regions, a shift which Gong et al. (2006) attribute to a positive phase of the WP (and therefore of the EAJ). Consequently, a stronger WP (EAJ) or poleward shift in the WP (EAJ) may lead to more Asian Dust loading and transport to the western North Pacific. The mean cross-Pacific trajectory of the Asian Dust transport parallels the mean trajectory of the EAJ, following the Pacific storm track, so a long-term shift in the mean latitudinal position or interannual variance of the EAJ would also alter the cross-Pacific path of the Asian Dust.

5 Conclusions

Interpretations of changes in large-scale climate patterns based on analyses of a single tree-ring chronology, a 'point source' location, would by themselves be highly questionable if not for the consistency of those interpretations with

previous research. Recent trends in the EAJ have been reported by many researchers (e.g. Seidel et al. 2008), and long-term trends in Tibetan ice core data have been interpreted as being related to EAJ trends noted in the twentieth century reanalysis data (Moore 2013). The upward trend in the running variance of the Taiwan tree-ring width data, and therefore in the EAJI 5YR and WPI 5YR reconstructions, may be caused by changes in the proximity of Taiwan to the EAJ core and WP dipole axis locations, changes in the strength/breadth of the EAJ core and WP pressure, or both. Similar analyses of ring width data in the same region, but poleward of the spring EAJ core location (e.g. central and northern Japan), are recommended.

Acknowledgments Our thanks to Mr. C.-L. Lin and the personnel of the Taiwan Forest Conservation Agency, also to C–S. Kang, Y.-H. Lan, S.-K. Huang, L.-S. Chiang, P.-Y. Chen, T.-T. Chen, C.-W. Yiu, and S.-W. Hsu for their assistance in the field and in the lab. Many of the figures were modified from images produced on the KNMI (Royal Netherlands Meteorological Institute) website (http://climexp.knmi.nl). Support for the Twentieth Century Reanalysis Project dataset is provided by the US Department of Energy, Office of Science Innovative and Novel Computational Impact on Theory and Experiment (DOE INCITE) program, and Office of Biological and Environmental Research (BER), and by the National Oceanic and Atmospheric Administration Climate Program Office. This research was partially funded by NSC Grant Numbers NSC 97-2627-M-002-023 and NSC 98-2627-M-002-011, and by the NSF Paleoclimate program, award ATM 04-02474.

References

Alibert C, Kinsley L (2008) A 170-year Sr/Ca and Ba/Ca coral record from the western Pacific warm pool: 1. What can we learn from an unusual coral record? J Geophys Res Ocean 113(C4):C04008. doi:10.1029/2006jc003979

Apipattanavis S, McCabe GJ, Rajagopalan B, Gangopadhyay S (2009) Joint spatiotemporal variability of global sea surface temperatures and global palmer drought severity index values. J Clim 22(23):6251–6267

Barnston AG, Livezey RE (1987) Classification, seasonality and persistence of low-frequency atmospheric circulation patterns. Mon Weather Rev 115(6):1083–1126

Berryman AA, Stenseth NC, Isaev AS (1987) Natural regulation of herbivorous forest insect populations. Oecologia 71(2):174–184. doi:10.1007/bf00377282

Bruijnzeel LA, Veneklaas EJ (1998) Climatic conditions and tropical, montane forest productivity: the fog has not lifted yet. Ecology 79(1):3–9

Buckley BM, Cook BI, Bhattacharyya A, Dukpa D, Chaudhary V (2005) Global surface temperature signals in pine ring-width chronologies from southern monsoon Asia. Geophys Res Lett 32(20):L20704. doi:10.1029/2005gl023745

Buckley BM, Duangsathaporn K, Palakit K, Butler S, Syhapanya V, Xaybouangeun N (2007) Analyses of growth rings of Pinus merkusii from Lao PDR. For Ecol Manage 253(1–3):120–127

Buckley BM, Anchukaitis KJ, Penny D, Fletcher R, Cook ER, Sano M, Le CN, Wichienkeeo A, Ton TM, Truong MH (2010) Climate as a contributing factor in the demise of Angkor, Cambodia. Proc Natl Acad Sci USA 107(15):6748–6752

Chang SC, Yeh CF, Wu MJ, Hsia YJ, Wu JT (2006) Quantifying fog water deposition by in situ exposure experiments in a mountainous coniferous forest in Taiwan. For Ecol Manage 224(1–2):11–18. doi:10.1016/j.foreco.2005.12.004

Charles CD, Cobb KM, Moore MD, Fairbanks RG (2003) Monsoon-tropical ocean interaction in a network of coral records spanning the 20th century. Mar Geol 201(1–3):207–222. doi:10.1016/s0025-3227(03)00217-2

Chiang JCH, Fang Y (2010) Was the North Pacific Wintertime climate less stormy during the mid-holocene? J Clim 23(14):4025–4037. doi:10.1175/2010jcli3510.1

Chu H-S, Chang S-C, Klemm O, Lai C-W, Lin Y-Z, Wu C-C, Lin J-Y, Jiang J-Y, Chen J, Gottgens JF, Hsia Y-J (2014) Does canopy wetness matter? Evapotranspiration from a subtropical montane cloud forest in Taiwan. Hydrol Process 28(3):1190–1214. doi:10.1002/hyp.9662

Cleveland WS, Devlin SJ (1988) Locally weighted regression: an approach to regression analysis by local fitting. J Am Stat Assoc 83(403):596–610

Compo GP, Whitaker JS, Sardeshmukh PD, Matsui N, Allan RJ, Yin X, Gleason BE Jr, Vose RS, Rutledge G, Bessemoulin P, Broennimann S, Brunet M, Crouthamel RI, Grant AN, Groisman PY, Jones PD, Kruk MC, Kruger AC, Marshall GJ, Maugeri M, Mok HY, Nordli O, Ross TF, Trigo RM, Wang XL, Woodruff SD, Worley SJ (2011) The twentieth century reanalysis project. Q J R Meteorol Soc 137(654):1–28. doi:10.1002/qj.776

Cook ER (1985) A time series analysis approach to tree ring standardization. The University of Arizona, Tucson

Cook ER, Peters K (1981) The smoothing spline: a new approach to standardizing forest interior tree-ring width series for dendro climatic studies. Tree-Ring Bull 41:45–53

Cook ER, Peters K (1997) Calculating unbiased tree-ring indices for the study of climatic and environmental change. Holocene 7(3):361–370. doi:10.1177/095968369700700314

Cook ER, Briffa KR, Shiyatov S, Mazepa V (1990) Tree-ring standardization and growth-trend estimation. In: Cook ER, Kariukstis LA (eds) Methods of dendrochronology: applications in the environmental sciences. International institute for applied systems analysis. Kluwer, Boston, pp 104–123

Cook ER, Meko DM, Stahle DW, Cleaveland MK (1999) Drought reconstructions for the continental United States. J Clim 12(4):1145–1162

D'Arrigo R, Smerdon JE (2008) Tropical climate influences on drought variability over Java, Indonesia. Geophys Res Lett 35(5):L05707. doi:10.1029/2007gl032589

D'Arrigo R, Villalba R, Wiles G (2001) Tree-ring estimates of Pacific decadal climate variability. Clim Dyn 18(3–4):219–224. doi:10.1007/s003820100177

D'Arrigo R, Allan R, Wilson R, Palmer J, Sakulich J, Smerdon JE, Bijaksana S, Ngkoimani LO (2008) Pacific and Indian Ocean climate signals in a tree-ring record of Java monsoon drought. Int J Climatol 28(14):1889–1901. doi:10.1002/joc.1679

D'Arrigo R, Wilson R, Tudhope A (2009) The impact of volcanic forcing on tropical temperatures during the past four centuries. Nat Geosci 2(1):51–56. doi:10.1038/ngeo393

D'Arrigo R, Palmer J, Ummenhofer CC, Kyaw NN, Krusic P (2011) Three centuries of Myanmar monsoon climate variability inferred from teak tree rings. Geophys Res Lett 38:L24705. doi:10.1029/2011gl049927

Dawdy DR, Matalas NC (1964) Statistical and probability analysis of hydrologic data, part III: analysis of variance, covariance and time series. In: Chow VT (ed) Handbook of applied hydrology, a compendium of water-resources technology. McGraw-Hill Book Company, New York, pp 8.68–68.90

Farjon A (2010) Handbook of the world's conifers, vol 1. Brill Academic Publishers, Leiden, pp 1–1111. doi:10.1163/9789047430629

Fritts HC (1976) Tree rings and climate. Academic Press, London

Ghil M, Allen MR, Dettinger MD, Ide K, Kondrashov D, Mann ME, Robertson AW, Saunders A, Tian Y, Varadi F, Yiou P (2002) Advanced spectral methods for climatic time series. Rev Geophys 40(1):3-1-41

Gong SL, Zhang XY, Zhao TL, Zhang XB, Barrie LA, McKendry IG, Zhao CS (2006) A simulated climatology of Asian dust aerosol and its trans-Pacific transport. Part II: interannual variability and climate connections. J Clim 19:104–122

Gong DY, Mao R, Shi PJ, Fan YD (2007) Correlation between East Asian dust storm frequency and PNA. Geophys Res Lett 34(14). doi:10.1029/2007gl029944

Grant AN, Bronnimann S, Ewen T, Nagurny A (2009) A new look at radiosonde data prior to 1958. J Clim 22(12):3232–3247

Hamed KH, Rao AR (1998) A modified Mann–Kendall trend test for autocorrelated data. J Hydrol 204(1–4):182–196. doi:10.1016/s0022-1694(97)00125-x

Holmes RL (1983) Computer-assisted quality control in tree-ring dating and measurement. Tree-Ring Bull 43:69–78

Hu C, Henderson GM, Huang J, Chen Z, Johnson KR (2008) Report of a three-year monitoring programme at Heshang Cave, Central China. Int J Speleol 37(3):143–151

Huang T-C (ed) (1994) Flora of Taiwan, second edition, vol 1. Editorial Committee of the Flora of Taiwan, Taipei

Ise T, Moorcroft PR (2008) Quantifying local factors in medium-frequency trends of tree ring records: case study in Canadian boreal forests. For Ecol Manage 256(1–2):99–105. doi:10.1016/j.foreco.2008.04.007

Ishii H, Ohsugi Y (2011) Light acclimation potential and carry-over effects vary among three evergreen tree species with contrasting patterns of leaf emergence and maturation. Tree Physiol 31(8):819–830. doi:10.1093/treephys/tpr079

Jhun JG, Lee EJ (2004) A new East Asian winter monsoon index and associated characteristics of the winter monsoon. J Clim 17(4):711–726

Kalnay E et al (1996) The NCEP/NCAR 40-year reanalysis project. Bull Am Meteorol Soc 77:437–471

Kistler R, Kalnay E, Collins W, Saha S, White G, Woollen J, Chelliah M, Ebisuzaki W, Kanamitsu M, Kousky V, van den Dool H, Jenne R, Fiorino M (2001) The NCEP-NCAR 50-year reanalysis: monthly means CD-ROM and documentation. Bull Am Meteorol Soc 82(2):247–267

Lai IL, Scharr H, Chavarria-Krauser A, Kusters R, Wu JT, Chou CH, Schurr U, Walter A (2005) Leaf growth dynamics of two congener gymnosperm tree species reflect the heterogeneity of light intensities given in their natural ecological niche. Plant, Cell Environ 28(12):1496–1505

Lai I-L, Chang S-C, Lin P-H, Chou C-H, Wu J-T (2006) Climatic characteristics of the subtropical mountainous cloud forest at Yuanyang Lake long-term ecological research site, Taiwan. Taiwania 51(4):317–329

Lau N-C (1988) Variability of the observed midlatitude storm tracks in relation to low frequency changes in the circulation pattern. J Atmos Sci 45(19):2718–2743

Lee YY, Lim GH, Kug JS (2010) Influence of the East Asian winter monsoon on the storm track activity over the North Pacific. J Geophys Res Atmos 115. doi:10.1029/2009jd012813

Letts MG, Mulligan M (2005) The impact of light quality and leaf wetness on photosynthesis in north-west Andean tropical montane cloud forest. J Trop Ecol 21:549–557. doi:10.1017/s0266467405002488

Lewis JM (2003) Ooishi's observation—viewed in the context of jet stream discovery. Bull Am Meteorol Soc 84(3):357–369. doi:10.1175/bams-84-3-357

Linkin ME, Nigam S (2008) The north pacific oscillation-west Pacific teleconnection pattern: mature-phase structure and winter impacts. J Clim 21(9):1979–1997

Lu J, Vecchi GA, Reichler T (2007) Expansion of the Hadley cell under global warming (vol 34, art no L06805, 2007). Geophys Res Lett 34(14):L14808. doi:10.1029/2007gl030931

Mann ME, Lee J (1996) Robust estimation of background noise and signal detection in climatic time series. Clim Change 33:409–445

Meko DM, Graybill DA (1995) Tree-ring reconstruction of Upper Gila River discharge. Water Resour Bull 31:605–616

Mildenberger K, Beiderwieden E, Hsia YJ, Klemm O (2009) CO_2 and water vapor fluxes above a subtropical mountain cloud forest—the effect of light conditions and fog. Agric For Meteorol 149(10):1730–1736

Mitchell TD, Jones PD (2005) An improved method of constructing a database of monthly climate observations and associated high-resolution grids. Int J Climatol 25(6):693–712

Miyamoto K, Okuda S, Inagaki Y, Noguchi M, Itou T (2013) Within- and between-site variations in leaf longevity in hinoki cypress (*Chamaecyparis obtusa*) plantations in southwestern Japan. J For Res 18(3):256-269. doi:10.1007/s10310-012-0346-1

Moore GWK (2013) Tibetan ice core evidence for an intensification of the East Asian jet stream since the 1870s. Atmos Sci Lett 14(4):235–242. doi:

Nakamura H (1992) Midwinter suppression of baroclinic wave activity in the Pacific. J Atmos Sci 49(17):1629–1642

Nigam S, Pyle J, Curry JA (2003) Teleconnections. Encyclopedia of atmospheric sciences. Academic Press, London

Park JS, Jhun JG, Kwon M (2010) Prominent features of large-scale atmospheric circulation during spring droughts over northeast Asia. Int J Climatol 30(8):1206–1214

Phipps RL (1982) Comments on interpretation of climatic information from tree rings, Eastern North America. Tree Ring Res 42:11–22

Pinheiro JC, Bates DM (2000) Mixed-effects models in S and S-plus. Statistics and computing. Springer, New York

Pumijumnong N, Eckstein D (2011) Reconstruction of pre-monsoon weather conditions in northwestern Thailand from the tree-ring widths of Pinus merkusii and Pinus kesiya. Trees-Struct Funct 25(1):125–132. doi:10.1007/s00468-010-0528-4

Pumijumnong N, Eckstein D, Sass U (1995) Tree-ring research on Tectona grandis on northern Thailand. Iawa J 16(4):385–392

Riviere G (2010) Role of Rossby wave breaking in the west Pacific teleconnection. Geophys Res Lett 37:L11802. doi:10.1029/2010GL043309

Sano M, Buckley BM, Sweda T (2009) Tree-ring based hydroclimate reconstruction over northern Vietnam from *Fokienia hodginsii*: eighteenth century mega-drought and tropical Pacific influence. Clim Dyn 33(2–3):331–340. doi:10.1007/s00382-008-0454-y

Seager R, Harnik N, Kushnir Y, Robinson W, Miller J (2003) Mechanisms of hemispherically symmetric climate variability. J Clim 16(18):2960–2978. doi:10.1175/1520-0442(2003)016<2960:mohscv>2.0.co;2

Seager R, Harnik N, Robinson WA, Kushnir Y, Ting M, Huang HP, Velez J (2005) Mechanisms of ENSO-forcing of hemispherically symmetric precipitation variability. Q J R Meteorol Soc 131(608):1501–1527. doi:10.1256/qj.04.96

Seidel DJ, Fu Q, Randel WJ, Reichler TJ (2008) Widening of the tropical belt in a changing climate. Nat Geosci 1(1):21–24. doi:10.1038/ngeo.2007.38

Shi JF, Cook ER, Lu HY, Li JB, Wright WE, Li SF (2010) Tree-ring based winter temperature reconstruction for the lower reaches of the Yangtze River in southeast China. Clim Res 41:169–175

Stokes MA, Smiley TL (1968) An introduction to tree ring dating. University of Chicago Press, Chicago

Thomson DJ (1982) Spectrum estimation and harmonic-analysis. Proc IEEE 70(9):1055–1096. doi:10.1109/proc.1982.12433

Tudhope AW, Chilcott CP, McCulloch MT, Cook ER, Chappell J, Ellam RM, Lea DW, Lough JM, Shimmield GB (2001) Variability in the

El Nino-Southern oscillation through a glacial-interglacial cycle. Science 291(5508):1511–1517. doi:10.1126/science.1057969

Urban FE, Cole JE, Overpeck JT (2000) Influence of mean climate change on climate variability from a 155-year tropical Pacific coral record. Nature 407(6807):989–993

Valladares F, Niinemets U (2008) Shade tolerance, a key plant feature of complex nature and consequences. Annu Rev Ecol Evol Syst 39:237–257

Wallace JM, Gutzler DS (1981) Teleconnections in the geopotential height field during the northern hemisphere winter. Mon Weather Rev 109(4):784–812

Wettstein JJ, Wallace JM (2010) Observed patterns of month-to-month storm-track variability and their relationship to the background flow. J Atmos Sci 67(5):1420–1437

Wigley TML, Briffa KR, Jones PD (1984) On the average value of correlated time series, with application in dendroclimatology and hydrometeorology. J Clim Appl Meteorol 23:201–213

Woollings T, Hoskins B, Blackburn M, Berrisford P (2008) A new Rossby wave-breaking interpretation of the North Atlantic Oscillation. J Atmos Sci 65(2):609–626

Wyka T, Robakowski P, Zytkowiak R (2008) Leaf age as a factor in anatomical and physiological acclimative responses of *Taxus baccata* L. needles to contrasting irradiance environments. Photosynth Res 95(1):87–99. doi:10.1007/s11120-007-9238-1

Yue S, Wang CY (2004) The Mann–Kendall test modified by effective sample size to detect trend in serially correlated hydrological series. Water Resour Manage 18(3):201–218. doi:10.1023/b:warm.0000043140.61082.60